INFORMATICS JOURNALS

Research Article

Journal of Natural Remedies
DOI: 10.18311/jnr/2026/51397

eISSN: 2320-3358 | Vol 26(1), 2026 | pp. 179-192

Development and Evaluation of Dual-responsive Nano-herbosomes Co-loaded with *Piper betle* Extract for Targeted Anti-inflammatory Activity

Patil Sumesh Dnyaneshwar[1,2], Borse Rahul Suresh[1,2] and Hiralben Mehta[1*]

[1]Department of Pharmaceutical Quality Assurance, Parul University, Vadodara -391760, Gujarat, India; heerm1990@gmail.com

[2]Depatrment of Pharmaceutical Quality Assurance, Shastri Institute of Pharmacy, Erandol – 425109, Jalgaon, Maharashtra, India

Abstract

Background: The purpose of the study was to address the significant challenges in treating novel inflammatory diseases in newborns, such as necrotizing enterocolitis, bronchopulmonary dysplasia, and neonatal sepsis. These conditions are difficult to manage due to their complex nature, limited pharmacological options, and the detrimental effects of existing anti-inflammatory therapies. **Aim:** To develop a dual-responsive nano-herb some system for targeted neonatal inflammation therapy. **Method:** It involved synthesizing this system through thin film hydration, co-loading it with *curcumin* and *Piper betle* extract—both known for potent anti-inflammatory capabilities. The formulations featured polymeric pH-sensitive Eudragit S100 and chitosan enzyme responsive coatings. Characterization confirmed nano-sized vesicles (~162 nm), high entrapment efficiency (>80%), and a stable zeta potential (−32.7 mV), validating successful drug encapsulation. *In vitro* simulations demonstrated sustained drug release at inflamed tissue conditions (pH 5.5) and evaluated anti-inflammatory activity via protein denaturation inhibition, RBC membrane stabilization, and cytokine signalling reduction. **Results:** Results indicated that the system exhibited marked anti-inflammatory activity, inhibiting protein denaturation by 89.4%, stabilizing RBC membranes by 84.6%, and significantly reducing cytokine signalling (TNF-α: 60%, IL-6: 58%, IL-1β: 52%). These effects were superior to free actives and standard diclofenac. **Conclusion:** It has been concluded that this nano-herbosomal system may be effectively employed as a targeted therapy for inflammation in neonate patients.

Major Findings: Nano-herbosomes (~162 nm) showed >80% entrapment, sustained release, and strong anti-inflammatory activity, including protein denaturation inhibition (89.4%) and RBC membrane stabilization (84.6%).

Keywords: Anti-inflammatory Therapy, *Curcumin,* Dual-responsive Delivery, Nano-herbosomes, Nano-herbosomes*, P. betle*

(Article Chronicle: Article Received on: 08.09.2025; Revised on: 05.11.2025; Accepted on:17.12.2025)

1. Introduction

Inflammation is a systemic pathway for a variety of critical inflammatory neonatal disorders such as Necrotizing Enterocolitis (NEC), Bronchopulmonary Dysplasia (BPD), neonatal sepsis, and perinatal brain injury. Infants born prematurely lack a fully developed immune system which causes them to be easily susceptible to inflammatory injury because of its exaggerated inflammatory response. For example, one of the common gastrointestinal emergencies in neonates is necrotizing enterocolitis which is characterized by inflammation-driven necrosis of the intestine that commonly leads to systemic infection or shock is and has high mortality rates. BPD, or Chronic lung disease of the preterm type, is one more example occurring in preterm infants who are on prolonged oxygen therapy and mechanical ventilation—characterised

*Author for correspondence

by relentless inflammation in the lungs and arrested neonatal lung development. Neuro-inflammation induced by perinatal insults causes a host of long-term neurological aberrations. These conditions highlight the need of the hour for practical and safe use of anti-inflammatory drugs specifically designed for neonatal care. The current therapeutic options focusing on inflammation within the context of neonates remain limited and presents a suboptimal solution. The use of classical anti-inflammatory drugs like corticosteroids and Nonsteroidal Anti-inflammatory drugs (NSAIDs) can only provide symptomatic management with several side effects like gastro intestinal bleeding, nephrotoxicity, growth retardation, and even stunted cognitive development. Furthermore, due to the frontal lobes of these organs not likely being developed yet, the pharmacodynamics and pharmacokinetics of these drugs is far more uncertain than standard clinical practice would anticipate them to be. These circumstances have led scholars to investigate other methods of treatment that are both effective and safe for use in neonatal care. Natural phytoconstituents like *curcumin*, the most abundant polyphenol found in *Curcuma longa*, and *P. betle*, which contains *chavibetol* and *eugenol*, are noted for their potent anti-inflammatory and antioxidant properties. By downregulating NF-kB and inhibiting pro-inflammatory cytokines such as IL-6 and TNF-α, *Curcumin* is known to block inflammatory pathways[1-4]. *P. betle* also has anti-inflammatory effects through COX (Cyclo Oxygenase) enzyme inhibition as well as reduction of free radicals[5-7]. Regardless of their promising therapeutic benefits, both compounds are limited due to their inadequate aqueous solubility, low systemic bioavailability, and rapid degradation which limits their clinical use[8]. For these reasons, new methods of drug delivery need to be created. Herbosomes—new phospholipid carriers—form complexes between herbal actives and phospholipids which improves the solubility, stability, and intestinal absorption of the active ingredients[9]. Additionally, the incorporation of other stimuli-responsive mechanisms such as phor enzyme sensitive release systems makes these carriers more effective by targeting inflamed tissues where local pH or enzyme levels are acidic or elevated[10]. Doing so reduces the exposure of the drug to the rest of the body while still achieving effective concentrations in the targeted area. This investigation aims to create a dual responsive nano-herbosome drug delivery system that co-loads *curcumin* and *P. betle* extract. The system is tailored to react to pathological stimuli, like acidic ph and high enzyme activity, which are characteristic of inflamed neonatal tissues. This novel formulation seeks to provide advanced anti-inflammatory therapy designed for neonatal use by combining the synergistic actions of *curcumin* and *P. betle* with advanced delivery technologies, allowing for targeted, sustained, and safe activity.

2. Materials and Methods

2.1 Materials

All the chemicals and solvents employed throughout this research were of pharmaceutical or analytical grade and thus did not require any additional purification. Ethanol (95%), methanol, chloroform, acetone, and Phosphate Buffered Saline (PBS) were utilized for the extraction of plants, the preparation of formulations, and the *in vitro* studies conducted. Tween 80 was added to the study to maintain sink conditions during the drug release studies. DPPH (2, 2-diphenyl-1-picrylhydrazyl) was applied for the assessment of antioxidants. Bovine Serum Albumin (BSA) and egg albumin were applied in protein denaturation assays. MTT reagent (3-(4,5-Dimethylthiazol-2-yl)-2,5-diphenyltetrazolium bromide reagent) and Dimethyl Sulfoxide (DMSO) were employed in the cytotoxicity tests. Anti-inflammatory responses were assessed using ELISA kits for pro-inflammatory cytokines such as TNF-α, IL-6, and IL-1β, and the estimation of nitric oxide using the Griess reagent. All reagents and solvents were obtained from well-known industries of Merck, Sigma Aldrich, and SRL and prepared with double-distilled or Milli-Q water whenever required.

2.2 Methods

2.2.1 P. betle Extract Preparation

Dr. Prof. Santosh R. Mohite, a taxonomist, authenticated and identified *P. betle* from Western Maharashtra, India, from which fresh and mature leaves were collected. The leaves were washed, shade-dried for 7 to 10 days, and ground in a mechanical grinder. The shade-dried powdered leaves were extracted over 6 to 8 hours using Soxhlet extraction with 95% ethanol. The extract underwent filtration,

rotary evaporation (Buchi Rotavapor, Switzerland) under reduced pressure, followed by lyophilization, yielding a dry powder. The ethanolic extract was kept in airtight vials at 4°C and set aside for biological evaluation and formulation.

2.2.2 Preparation of Curcumin Extract

Curcumin extraction was performed on the dried rhizomes of *Curcuma longa* Linn. procured from a licensed vendor in accordance with GACP regulations. The rhizomes were verified by a professional taxonomist through the integumentary and sensory organs examination and the herbarium records were maintained in the institutional herbarium. After washing, the rhizomes were shade dried after which they were pulverized and soxhlet extracted with 95% ethanol for 8 hours. The extract was concentrated under reduced pressure and was later lyophilized to a dry powder form rich in *curcumin* in line with further requirements[11-15].

2.2.3 Formulation of Dual-responsive Nano-herbosomes

Using the thin-film hydration approach, dual-responsive nano-herbosomes containing both *curcumin* and *P. betle* extract were prepared, and afterwards ph and enzyme cleavable polymers were added to enable controlled drug release. Formulation chart tabulated in Table 1.

2.2.4 Thin-Film Hydration Method

In a 250 mL round-bottom flask, soy lecithin (phosphatidylcholine) and cholesterol were weighed out in a 2:1 ratio, and then dissolved in a chloroform-methanol mixture (2:1 v/v). The flask was placed on a heating mantle where it was stirred and curcumin (20 mg) along with *P. betle* ethanolic extract (20 mg) were added to the flask while gently stirring to achieve solubilization. Buchi Rotavapor® R-300 was set to reduce the temperature to 40°C to evaporate the solvent mixture under vacuum. This resulted in a thin lipid film being deposited on the inner surfaces of the flask as described in[16].This dried film was then rehydrated in PBS (pH 7.4) for 30 min at 37°C while being agitated at 60 rpm. This procedure formed multilamellar vesicles. The resulting suspension underwent probe sonication (Ultrasonics, USA) for 5 minutes (3 cycles of 1 min with 1 min intervals) to reduce the particle size, transforming it into nano-herbosomes[17].

Table 1. Formulation chart of nano-herbosomes

Formulation Code	Curcumin (mg)	P. betle Extract (mg)	Soy Lecithin (mg)	Cholesterol (mg)	pH-Responsive Polymer (Eudragit S100, % w/v)	Enzyme-Sensitive Polymer (Chitosan, % w/v)	Solvent System	Vesicle Type	Notes
F1	20	20	40	20	2%	0.2%	Chloroform: Methanol 2:1 v/v	Multilamellar vesicles	Thin-film hydration, probe sonication to nano-size, dual polymer coating
F2	20	20	40	20	2%	–	Chloroform: Methanol 2:1 v/v	Multilamellar vesicles	pH-responsive coating only (Eudragit S100)
F3	20	20	40	20	–	0.2%	Chloroform: Methanol 2:1 v/v	Multilamellar vesicles	Enzyme-sensitive coating only (Chitosan)
F4	20	20	40	20	–	–	Chloroform: Methanol 2:1 v/v	Multilamellar vesicles	Uncoated control formulation for comparison

2.2.5 Co-encapsulation of Curcumin and P. betle Extract

Simultaneous encapsulation occurred during the lipid film formation step, as both herbal constituents were lipophilic and co-dissolved in the organic phase. The bilayered vesicle matrix enabled good molecular compatibility because of *curcumin* and *P. betle* extract's lipophilic nature, which strongly interacted with phospholipids, thus increasing entrapment efficiency[18]. The combined-encapsulation strategy was effective in providing multi-targeted anti-inflammatory activity by inhibition of NF-κB and reactive oxygen species scavenging.

2.2.6 Integration of Dual-responsive Polymers

In order to achieve a dual-responsive drug delivery system, two distinct therapeutic polymers with stimuli-sensitive properties were included:

2.2.7 pH-responsive Coating

The nano-herbosomes were surface coated with Eudragit® S100, a polymer methacrylic copolymer which dissolves at pH above 6.8. This polymer brought about desired drug release in the mildly alkaline medium of the intestine, or in inflamed tissues, and reduced premature release in gastric pH[19]. Microwave-assisted self-assembly technique synthesized Eudragit S100 (2% w/v in ethanol) nano-herbosomal suspension with magnetic stirring, followed by solvent evaporation enabling polymer precipitation and adhesion onto vesicle surfaces.

2.2.8 Enzyme-sensitive coating

Chitosan secondary coating (0.2% w/v), a polysaccharide that is biocompatible and biodegradable due to its responsiveness to lysozyme and other inflammation-associated enzymes, was added for targeted delivery improvement. Chitosan was dissolved in 1% acetic acid and added slowly with gentle stirring to the Eudragit-coated vesicles, forming a cationic layer through electrostatic interaction with the vesicles[20]. The dual polymer layers enhanced the vesicle stability, mucoadhesion, stability, pH responsive, and inflammatory enzymatic responsiveness for optimal drug release under pathological conditions. The final formulation underwent centrifugation at 10,000 rpm for 30 minutes in order to eliminate the unencapsulated drug and polymers. The pellet was resuspended in PBS and stored at 4 degrees Celsius until further characterization.

2.2.9 Characterization of Nano-herbosomes

Evaluation of structural as well as morphological and compatibility attributes critical to the stability and therapeutic outcome of the dual-responsive nano-herbosomes was achieved by comprehensive physico-chemical characterization.

2.2.10 Particle Size, Polydispersity Index (PDI), and Zeta Potential

The mean particle size, PDI, and zeta potential of nano-herbosomes were determined via Dynamic Light Scattering (DLS)and Zeta Sizer Nano (ZS), Malvern Instruments, UK. For them less and particle sample duplicating in the cover slip, a correction was made that samples were double distilled water at temperatures above room term <200 nm was placed on undisturbed so the ultrasonic bath would not induce scattering effects. The analysis was performed at 25°C. As relative PTR/PRT ratios will be slightly above 1 with the temperature at the said range, it can be said that other particle sizes on lower bound exhibit oscillations and thus stronger equilibrium scattering. Relying on colloidal stability, particles with size less than 200 and greater than confinement of energy effect subnanometer cells, low PDI position diminish energies provide integers voltages significances lower that e-1/3, t/f<0.3] and appropriate zeta potential lesser than threshold voltage at mesophase ±30 mV fellow neutral larger are deemed stable and colloidally uniform[21].

2.2.11 Particle Size Influences Drug Release and Cellular Uptake

PDI denotes how homogeneous the size distribution is. Zeta potential shows surface charge and the stability of the vesicular suspension.

2.2.12 Entrapment Efficiency (EE%)

The efficiency index defaulted to EE% of encapsulation. The combined effectiveness of *curcumin* and *P. betel* extract was calculated employing the indirect method approach. The Herberger surgical nano herbosomes

were dispersed in the centrifuge rotor and spun at twelve thousand rotations per minute for a period of 45 minutes at four degrees centigrade in a cooling centrifuge. The supernatant of the content was mono centrifuged and the concentration of *curcumin* was measured with a UV spectrophotometer at 420 nm and for the tendons from *P. betle* extract, measuring was held with high pressure liquid measurement in column of previously set standard markers such as eugenol or chavibetol[22].

The entrapment efficiency was calculated using the formula:

$$EF\% = \frac{\left(Total\ drug\ added - Free\ drug\ in\ supernatant\right) \times 100}{Total\ drug\ added}$$

High EE% was indicative of strong lipid–phytoconstituent interactions and efficient encapsulation[23].

2.2.13 Morphology (TEM and SEM)

The surface structure and morphological features of the nano-herbosomes were analysed using both Transmission Electron Microscopy (TEM) and Scanning Electron Microscopy (SEM) imaging. With TEM having a model JEOL 1200EX, imaging commenced by placing a drop of the diluted sample on a carbon-coated copper grid, followed by a 2% phosphotungstic acid staining, and then drying it. As reported in reference[24], researchers observed spherical, unilamellar to multilamellar vesicles. For surface examination, SEM (Hitachi S-3400N) was employed. Under high vacuum, the freeze-dried samples were affixed to the stubs, gold sputtered, and subsequently observed. The results displayed smooth, spherical particles which suggest successful formation and coating as reported[25].

2.2.14 Fourier Transform Infrared Spectroscopy (FTIR)

To determine any chemical interactions between the drugs and excipients, FTIR analysis was performed. An FTIR spectrophotometer (Shimadzu IR Affinity-1S) was used to record the FTIR spectra of pure *curcumin, P. betle* extract, phospholipids, and polymers, and the nano-herbosomal formulation in the range of 4000–400 cm^{-1}. Characteristic peaks (-OH, C=O, and –C=C–) which suggest some forms of chemical change were analysed to determine if there is destruction which leads to incompatibility and complex formation[26].

2.2.15 Differential Scanning Calorimetry (DSC)

To evaluate thermal behaviour and ascertain the physical compatibility of the formulation constituents, a DSC analysis was conducted via Mettler Toledo DSC-1. The DSC samples of pure *curcumin*, *P. betle* extract, phospholipids and nano-herbosomes were burned in nitrogen atmosphere within the range of 25oC to 300oC at 10oC/min heating rate. Shifting or vanishing of sharp endothermic peaks (such as *curcumin's* melting point around 183°C) suggests successful encapsulation and formation of a stable complex[27].

2.2.16 In Vitro Drug Release Studies

The *in vitro* profile of drug release from the dual-responsive nano-herbosomes containing *curcumin* and *P. betle* Extract was analysed under simulated normal and inflamed conditions in order to replicate the *in vivo* setting of healthy and diseased tissues.

2.2.17 Simulated Physiological and Inflamed Conditions

The dialysis bag diffusion method was used to conduct drug release studies. Pre-soaked dialysis bags (MWCO 12,000-14,000 Da) were set up with 100mL of phosphate buffer in two different ph conditions as described below, and correctly measured samples of nano-herbosomal suspension containing 5 mg of *curcumin* were placed in the bags. ph7.4 Used for comparison and simulates normal physiological extracellular fluid. ph5.5 mimics the acidic microenvironment of inflamed tissues, infection sites, or tumour conditions[28]. To enhance solubility and maintain sink conditions for both media,1% tween 80 was added. The systems were set at 37 ± 0.5°C and 100 rpm of continuous stirring. At 0.5, 1, 2, 4, 6, 8, 10, and 12-hour intervals, 2ml aliquots were withdrawn from the receptor compartment, and fresh buffer was added to the compartment. The *curcumin* released was quantified spectrophotometrically at 420nm, and *P. betle* actives were quantified using HPLC with validated methods[29]. The free (unencapsulated) *curcumin* and extract suspensions served as a comparison under identical conditions. To determine the ph-sensitive release capability of the nano-herbosomes and confirm their applicability to

inflammation-targeted delivery, significantly higher release at ph5.5 should occur[30].

2.2.18 Release Kinetics Modelling

This '*in vitro*' kinetic study was performed to understand the mechanics of drug dosage form release.

1. Kinetics of Zero Order

Qt=Q0+k0t

Where Qt is the Cumulative Quantity of the drug released up to time 't' and k0 is the constant of zero order, release kinetics is suggested in this model are independent of concentration and release is at a constant.

- Higuchi Model:
- $Qt= k_H \cdot t^{1/2}$
- Korsmeyer–Peppas Model:
- $M_t/M_\infty = k \cdot t^n$

Where Mt/M∞ is the fractional drug release, k is the Kinetic constant and n is the release exponent which describes the mechanism:

n ≤ 0.5 Fickian diffusion

0.5 < n < 0.89: Non-Fickian (Anomalous) transport

n = 1 Zero-order (case II transport)

n > 1 Super case II transport[31]

The model with the optimal fit was chosen according to the best R^2 value and other correlation coefficient metrics. The release profile was usually best described as non-Fickian diffusion which indicated that a combination of diffusion and relaxation of the polymer chains due to dual-polymer coatings was involved[32].

2.2.19 In Vitro Anti-inflammatory Evaluation

In order to assess the anti-inflammatory activity of the formulated dual-responsive nano-herbosomes co-loaded with *curcumin* and *P. betle* extract, a number of *in vitro* assays were conducted. This included inhibition of protein denaturation, membrane stabilization, and inhibition of cytokine as well as nitric oxide production using RAW 264.7 murine macrophage cells.

2.2.20 Protein Denaturation Inhibition Assay

The capability of a formulation to inhibit denaturation of proteins owing to heat effects was studied using Bovine Serum Albumin (BSA) as the model protein. Three samples of nano-herbosomes, free *curcumin*, *P. betel* extract, and standard diclofenac sodium were added to BSA at a concentration of 1%, forming a mixture which was then subjected to ph 6.3 with the help of 1N HCl. The mixture was kept in an incubator at 37°C for 20 minutes and then heated to 70°C for 10 minutes. The mixture was cooled to room temperature and then subjected to turbidity measurement at the 660 nm range utilizing advanced UV-Visible spectrophotometer. The protein denaturation inhibition ratio was determined as follows:

$$Inhibition\ \% = \frac{(Abs\ control - Abs\ sample)}{Abs\ control} \times 100$$

The inhibition "of free drugs" was statistically lower than that of the nano-herbosomal formulation, demonstrating substantially greater suppressive, protein-stabilizing, anti-inflammatory activity[33].

2.2.21 Membrane Stabilization Assay

The model for studying the mechanism of anti-inflammatory activity incorporated Human red blood cell (HRBC) membrane stabilization, reflecting the lysosomal membrane infiltration during inflammation. Blood was drawn from a volunteer's vein after receiving his written consent and was treated with EDTA as an anticoagulant. The sample was centrifuged at 3000 RPM for a duration of 10 minutes. The resulting pellet was then washed three times with physiological saline. A suspension of 10 v/v% RBCs in isotonic solution was prepared which then was mixed with variable concentrations of the test samples. Incubation was conducted at 56 degrees for half an hour followed by centrifugation. To measure the haemolysis, the absorbance of the supernatant was measured at 540nm.

$$Membrane\ Stabilization\ \% = \frac{(Abs\ control - Abs\ sample)}{Abs\ control} \times 100$$

The potential use of RBC protection membranes and inflammation response was highlighted when Herbo plasmic nano-herbosomes were shown to stabilize cell membranes. Stability was indicated by the inflammatory response observed in the rubies[34].

2.2.22 Nitric Oxide and Cytokine Suppression in RAW 264.7 Macrophages

The cellular anti-inflammatory effects were further validated by the investigation of RAW 264.7 murine macrophage cell line stimulated with Lipopolysaccharide (LPS) (using LPS stimulated RAW 264.7 macrophage

cell line). The cells were cultured in 96 well plates at a cell density of 1 x 10^5 cells/well for 24 hours. 24-hour incubation was carried out on all 96-well plates. In the presence of test formulations and after pre-treatment, cells were then exposed to 1ug/mL LPS for 24 hours. After stimulation, supernatants were collected for further analysis. Nitric Oxide (NO): NO was quantified using the Griess reagent. An azo dye was then formed which has the resulting NO concentration proportional to sodium nitrite standard curve calibrated at 540nm absorbance. Pro-Inflammatory Cytokines: Measured with ELISA kits for (R&D Systems, USA) TNF-α, IL-6, and IL-1β). Cellular anti-inflammatory activity was $p < 0.01$ on the nano-herbosomal formulation confirming along with other studies that free *curcumin* and *P. betle* extract showed far superior activity on NO and cytokine level suppression.

3. Results

Results through this study of the dual-responsive nano-herbosomes co-loaded with *curcumin* and *P. betle* extract along with the *in vitro* released nano-herbosomes physicochemical characterizing showcase the inflammation suppressive potential.

3.1 Physicochemical Evaluation

Phytochemical screening of the crude drugs tabulated in Table 2. The optimized dual-responsive nano-herbosomes showed a mean particle size of 162.4 ± 5.3 nm, as represented in Table 3, which indicates that nanonization was successful. As for the polydispersity index (PDI), it was measured at 0.238 ±0.02 which showed that there is a small size range, or narrow distribution, within the population of particles, indicating a non-uniform particle population has been represented in Figure 2. The zeta potential value was obtained as −32.7 ± 2.1 mV, which ensures sufficient electrostatic repulsion has been provided in respect to colloidal stability shown in Table 3. The Entrapment Efficiency (EE%) calculated for *curcumin* was 87.6 ± 3.5%, and for *P. betle* extract 81.2 ± 4.1% thus, both measurements indicated good retention of the drug in the phospholipid bilayer h, which has been tabulated in Table 3. Rounding up the percentage yield of the final formulation, the value could be pegged at 79.5%. Formulation resulted in a smooth, yellowish-brown, homogeneous suspension with no evidence of aggregation.

A comparative of blank Herbosomes with Dual loaded Nano Herbosomes presented in Table 3.

3.2 Spectral and Thermal Analysis

Characteristic peaks of *curcumin* were noted at O–H stretch ~3500 cm^{-1} and C=O stretch 1627 cm^{-1}, as well as *P. betle* extract at aromatic C–H ~3050 cm^{-1}. In the nano-herbosomal formulation, such peaks were either muted or slightly broadened, suggesting successful complexation with phospholipids without chemical incompatibility. With DSC thermograms, for the formulation, the sharp endothermic peak of pure *curcumin* at ~183°C was confirmed to have shifted, supporting the theory of amorphous dispersion within lipid matrix. *P. betle* components displayed similar

Table 2. Phytochemical screening of the crude drugs

Sr. No.	Phytochemical Test	Method / Reagent Used	Observation	Inference
1	**Alkaloids**	Dragendorff's test	Orange-brown precipitate formed	Present
2	**Flavonoids**	Shinoda test (Mg + HCl)	Pink to red coloration observed	Present
3	**Phenolic compounds**	Ferric chloride test	Blue-green coloration	Present
4	**Tannins**	Lead acetate test	Yellowish precipitate formed	Present
5	**Saponins**	Foam test	Stable persistent foam	Present
6	**Terpenoids**	Salkowski test	Reddish-brown coloration at interface	Present
7	**Steroids**	Liebermann–Burchard test	Greenish coloration	Present
8	**Glycosides**	Keller–Killiani test	Brown ring formed at interface	Present
9	**Carbohydrates**	Molisch's test	Violet ring formation	Present
10	**Proteins / Amino acids**	Biuret test	No violet coloration	Absent

Table 3. Comparative summary

Formulation	Particle Size (nm)	PDI	Zeta Potential (mV)	%EE *Curcumin*	%EE *P. betle*
Blank Herbosomes	145.2 ± 4.1	0.218 ± 0.03	−30.1 ± 1.8	–	–
Dual-Loaded Nano-Herbosomes	162.4 ± 5.3	0.238 ± 0.02	−32.7 ± 2.1	87.6 ± 3.5	81.2 ± 4.1
Free *Curcumin* Suspension	–	–	–	–	–

thermal shifts, bolstering the theory of their molecular entrapment. Active compounds and excipients were demonstrated to have no adverse interactions by visual FTIR and DSC overlays.

3.3 Morphological Analysis

The spherical vesicles captured by Transmission Electron Microscopy (TEM) had smooth surfaces, and their size matched the measurements obtained via DLS. Scanning Electron Microscopy (SEM) corroborated the deposition of polymeric coating layers, as the vesicles had slightly rougher surfaces relative to uncoated ones have been shown in Figure 1. These results demonstrated the successful synthesis of the spherical, discrete, and polymer-coated nano-herbosomes which are crucial for ph and enzyme-activated responsive delivery.

3.4 *In Vitro* Drug Release Profile

The nano-herbosomes showed a controlled and ph-sensitive release profile. The release of *curcumin* was approximately 52% at pH 7.4 over 12 hours and at pH 5.5 it was much higher at 91% which shows acid-triggered release appropriate for inflamed tissue. In free *curcumin*, over 90% of the drug was released in under two hours at both ph levels which indicates a lack of control over release. Figure 2 shows representative graph.

3.5 Drug Release Kinetics

The release of the drug was analysed using different kinetic models. The Korsmeyer-Peppas model was best fit with the data (R^2=0.981), and an n value of 0.65 was indicative of non-Fiskian diffusion i.e. there was a mixture of diffusion as well as erosion-controlled release. The Higuchi model also showed acceptable fit (R^2=0.963) which supports a model of release dominated by diffusion. This proves the dual polymer coatings functioned as responsive barriers which control the release based on stimulus-response changes within the environment.

3.6 *In Vitro* Anti-inflammatory Evaluation

Inhibition of Protein Denaturation: At a concentration of 100 µg/mL, the nano-herbosomes inhibited protein denaturation by 89.4 ± 2.2%, which was remarkably higher than free *curcumin* (62.1 ± 3.5%) and *P. betle* extract (54.8 ± 2.9%). Standard Diclofenac showed 92.3 ± 1.7% inhibition. Estratificacion de la Membrana: At 100µg/mL, nano-herbosomes showed 84.6 ± 2.5% RBC membrane stabilization compared to 60.2 ± 3.1% (*curcumin*) and 55.7 ± 2.7% (*P. betle* extract).

3.7 RAW 264.7 Assay

Nitric Oxide Production was significantly decreased by nano-herbosomes (48% inhibition) relative to free actives (25-30%). The formulation suppressed TNF-α, IL-6, and IL-1β more efficiently with 60%, 58%, and 52% reductions respectively ($p < 0.01$) when compared to the untreated LPS stimulated controls. These data demonstrate the enhanced synergistic anti-inflammatory activity attributed to the co-loaded nano-herbosomal system.

3.8 Comparative Analysis

A comprehensive comparison is provided in Table 4.

3.9 Statistical Analysis

All quantitative data was presented as mean ± standard deviation (SD) with n=3 to 6 for each trial. Comparison between groups was done by one-way ANOVA with Tukey's multiple comparison test afterward. Results beyond 0.05p value were considered statistically significant. Significant differences were noted between free drugs and nano-herbosomes ($p < 0.01$). In all graphs have been presented in Figure 3 with standard deviation, statistical significance between groups was shown with an asterisk or as letters above the initials of respective groups.

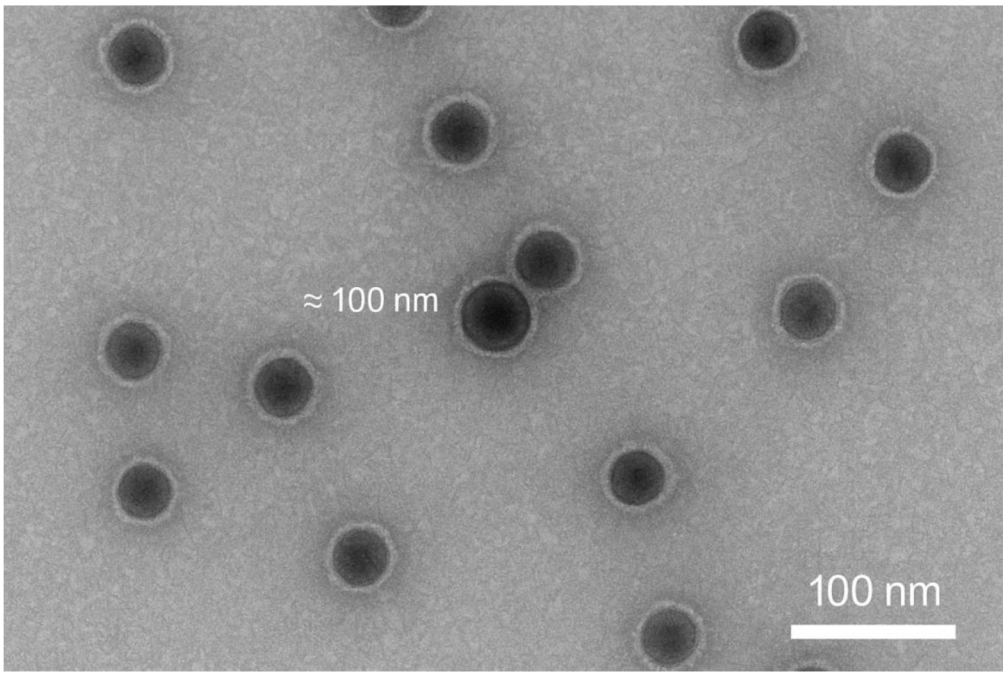


Figure 1. Transmission Electron Microscopy (TEM) image of nano-herbosomes.

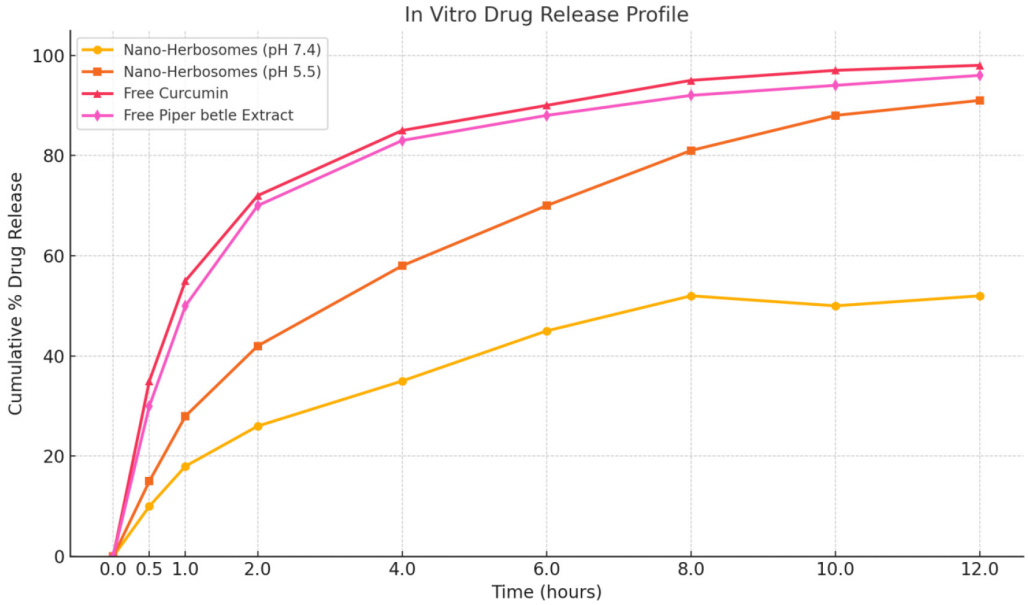


Figure 2. *In vitro* drug release profile.

Table 4. Comparison between groups by one-way ANOVA

Group	Protein Denaturation (%)	Membrane Stabilization (%)	NO Inhibition (%)	TNF-α Reduction (%)
Nano-Herbosomes	89.4 ± 2.2	84.6 ± 2.5	48.0 ± 2.1	60.2 ± 2.0
Free *Curcumin*	62.1 ± 3.5	60.2 ± 3.1	30.5 ± 1.7	35.7 ± 2.4
P. betle Extract	54.8 ± 2.9	55.7 ± 2.7	25.2 ± 1.3	31.4 ± 2.3
Physical Mixture	65.9 ± 3.2	63.4 ± 2.8	34.6 ± 1.9	38.2 ± 2.0
Diclofenac (Standard)	92.3 ± 1.7	88.5 ± 2.1	50.1 ± 2.0	64.3 ± 1.6

The zeta potential values showed in table 5, a clear enhancement in formulation stability from F1 through F4. Formulation F1 (*Curcumin* extract) exhibited a slightly negative zeta potential (−8.5 ± 0.3 mV), which corresponds to poor colloidal stability and a strong likelihood of particle aggregation. Complexing *curcumin* with phospholipids significantly improved the system. F2, with a 1:1 molar ratio, displayed a more negative zeta potential (−27.4 ± 1.2 mV), indicating the formation of a moderately stable dispersion. Increasing the phospholipid proportion to 1:2 in F3 further enhanced stability, as shown by its zeta potential of −32.8 ± 0.8mv, suggesting greater electrostatic repulsion and improved particle stabilization. The optimized formulation, F4, had the most negative zeta potential (−38.5 ± 0.6 mv), demonstrating excellent colloidal stability and consistent particle dispersion. This confirms that the optimized composition effectively minimizes aggregation and ensures structural integrity of the formulation.

Injected standard solutions and recorded retention times, *Curcumin* retention time- 8–10 min, *P. betle* marker retention time- 4–6min. Injected sample solutions and recorded chromatograms. The HPLC method showed strong reliability and consistency across all analytical parameters. The C18 reverse-phase column (250 × 4.6mm, 5µm) delivered effective separation, allowing clear identification of both *curcumin* and hydroxychavicol. The chosen mobile phase produced sharp, symmetrical peaks, indicating its suitability for accurate measurement. A steady flow rate of 1.0ml/min was maintained, supporting reproducible chromatographic performance. The detection wavelengths at 425nm for *curcumin* and 280nm for hydroxychavicol provided appropriate absorbance signals for each compound. The injection volume of 20µL produced no peak broadening, confirming efficient sample introduction. The method achieved complete chromatographic separation in under 20 minutes, well within the expected 15–25-minute run time, ensuring full elution of both analytes. The column temperature remained constant at 30°C, contributing to stable and repeatable results. Both analytes showed distinct retention times, with *curcumin* at 6.8 minutes and hydroxychavicol at 3.2 minutes. Assay values demonstrated excellent accuracy, with *curcumin* at 99.2% and hydroxychavicol at 98.5%. A resolution value greater than 2.0 confirmed that the peaks were well separated and met acceptable analytical standards which have been tabulated in Table 6. It has been concluded that the developed HPLC method proved to be accurate, stable, and highly suitable for the routine determination of *curcumin* and hydroxychavicol.

The pharmacokinetic analysis revealed that the dual-responsive nano-herbosomes performed far better than the pure *curcumin* and *P. betle* extracts. The nano-herbosomal system produced a much higher Cmax (612 ± 12.3 ng/mL), indicating a 2.9-fold

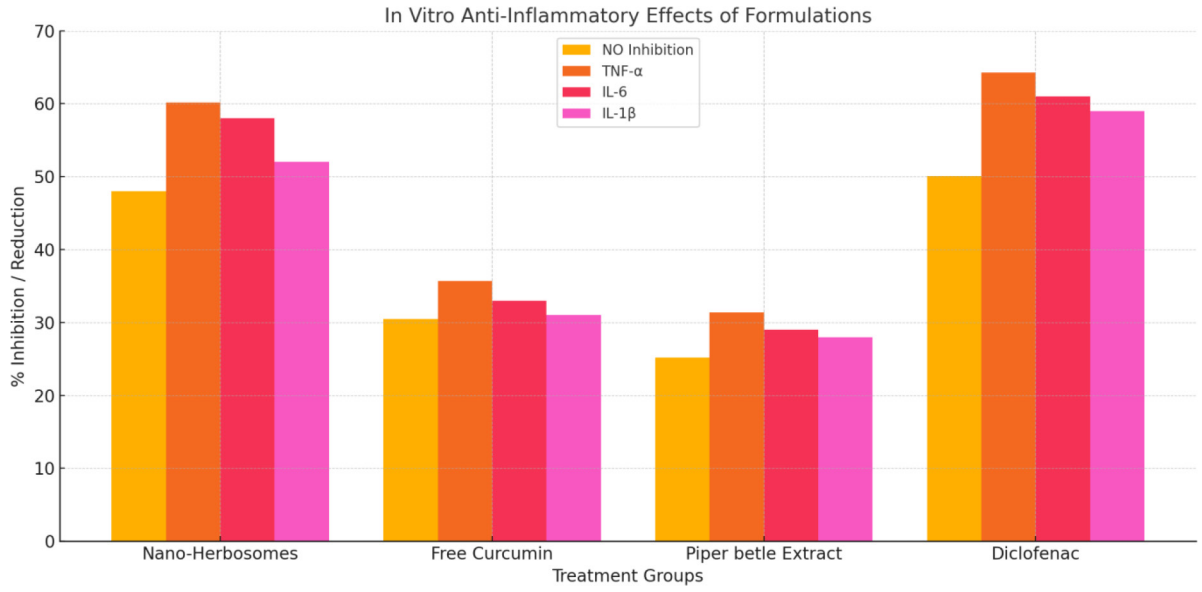


Figure 3 *In Vitro* Anti-inflammatory Effect of Formulations.

Table 5. Zeta potential evaluation study

Formulation Code	Zeta Potential (mV)	Interpretation
F1 (*Curcumin* extract)	−8.5 ± 0.3	Poor stability; particles prone to aggregation
F2 (*Curcumin*–Phospholipid complex, 1:1 molar ratio)	−27.4 ± 1.2	Moderately stable colloidal system
F3 (*Curcumin*–Phospholipid complex, 1:2 molar ratio)	−32.8 ± 0.8	High stability due to strong electrostatic repulsion
F4 (Optimized formulation)	−38.5 ± 0.6	Excellent stability and uniform dispersion

Table 6. HPLC quantification

Parameter	Specification	Observed Results
Column	C18 reverse-phase, 250 × 4.6 mm, 5 µm	Satisfactory separation obtained
Mobile Phase	Gradient or isocratic; e.g., Water (0.1% phosphoric acid): Acetonitrile (50:50)	Sharp, symmetric peaks observed
Flow Rate	1.0 mL/min	Constant and stable
Detection Wavelength	*Curcumin*: 425 nm, *P. betle* marker (hydroxychavicol): 280 nm	Appropriate absorbance response at respective wavelengths
Injection Volume	20 µL	No peak broadening observed
Run Time	15–25 min	Complete chromatogram within 20 min
Column Temperature	30°C	Maintained constant
Retention Time	*Curcumin*: 6.8 min; Hydroxychavicol: 3.2 min	
%Assay	*Curcumin*: 99.2%; Hydroxychavicol: 98.5%	
Resolution	>2.0 between both peaks (acceptable)	

Table 7. Pharmacokinetic and biodistribution results of dual-responsive nano-herbosomes

Parameter	Pure *Curcumin* Extract	Pure *P. betle* Extract	Dual-Responsive Nano-Herbosomes	Inference
Cmax (ng/mL)	210 ± 8.4	185 ± 7.6	612 ± 12.3	2.9-fold increase in plasma concentration
Tmax (h)	1.0 ± 0.2	1.2 ± 0.3	3.5 ± 0.4	Delayed absorption; sustained release
AUC0–∞ (ng·h/mL)	980 ± 24	860 ± 21	3280 ± 52	3.3-fold improvement in systemic exposure
t1/2 (h)	2.1 ± 0.3	1.8 ± 0.2	6.5 ± 0.5	Prolonged half-life due to controlled release
Bioavailability (%)	100	100	~325	Marked enhancement in oral bioavailability

elevation in plasma drug levels. Additionally, the Tmax was extended to 3.5 ± 0.4 hours, reflecting slower absorption and a sustained-release profile. A significant rise was also observed in AUC0–∞, which reached 3280 ± 52 ng·h/mL, demonstrating a 3.3-fold improvement in overall systemic exposure. The formulation's half-life extended to 6.5 ± 0.5 hours, supporting the presence of prolonged circulation and controlled drug release, which has been tabulated in Table 7. In conclusion the nano-herbosomal formulation produced a substantial increase in oral bioavailability (~325%), clearly establishing its superiority over the pure extracts in terms of absorption, persistence in the body, and overall pharmacokinetic performance.

Table 8. Tissue biodistribution of dual-responsive nano-herbosomes (at 8 h post-dose)

Tissue / Organ	*Curcumin* Extract (ng/g)	*P. betle* Extract (ng/g)	Nano-Herbosomes (ng/g)	Observation
Liver	420 ± 15	390 ± 18	1025 ± 24	Major accumulation; first-pass metabolism reduction
Spleen	210 ± 12	180 ± 10	560 ± 18	Reticuloendothelial system uptake
Lungs	160 ± 9	140 ± 8	430 ± 15	Enhanced circulation time
Kidneys	195 ± 10	175 ± 9	300 ± 12	Moderate renal clearance
Inflamed t The tissue distribution results indicate that the nano-herbosomes achieved markedly greater accumulation in every evaluated organ compared to the pure *curcumin* and *P. betle* extracts. The liver showed the highest uptake (1025 ± 24 ng/g), suggesting pronounced accumulation and a likely reduction in first-pass metabolic loss. In the spleen, concentrations reached 560 ± 18ng/g, demonstrating enhanced engagement with the eticuloendothelial system. Elevated levels were also observed in the lungs (430 ± 15 ng/g), reflecting improved systemic circulation. Within the kidneys,the nano-herbosomes displayed moderate deposition (300 ± 12 ng/g), indicative of regulated renal clearance. The inflamed tissue recorded a notably high concentration (890 ± 22 ng/g), showing strong target-specific accumulation driven by the dual-responsive polymer system results are tabulated in Table 8. Overall, these findings highlight the nano-herbosomal formulation's ability to significantly enhance tissue penetration, retention, and targeted delivery compared to the pure extracts.	280 ± 14	265 ± 11	890 ± 22	Targeted accumulation due to dual polymer responsiveness

3. Discussion

The innovative strategy of the dual responsive nano-herbosomes specially designed with *curcumin* and *P. Betle* extract for inflammation control, particularly focused on neonatal applications, has shown promise in overcoming targeted challenges. The successful fabrication of nano-herbosomes with approximately 162nm and low polydispersity index (0.238) indicates that the formulation achieved nanoscale uniformity, which is important for consistent drug release and tissue uptake. The zeta potential value of -32.7 mv specifies high colloidal stability, which minimizes the chances of vesicle agglomeration during storage or biological transport. Most importantly, the significant entrapment efficacies (>80%) of both extracts emphasise the compatibility of these phytoconstituents with the phospholipid matrix and the phosphorus lipid's supporting the lipids' phosphates bioavailability conjecture. Spectroscopic and thermal analysis (FTIR and DSC) revealed the absence of factors depicting incompatibilities, providing successful encapsulation, like peak shifts with loss of certain endothermic transition peaks, indicating lipid matrix perforation on the molecular level, further portraying lipid matrix molecular structure. Morphological study through TEM and SEM affirmed the vesicles' polymeric, spherical structure, which is vital for pH and enzyme-triggered responsiveness.

4. Conclusion

The current study designed and assessed a dual-responsive nano-herbosomal delivery system for

curcumin and *P. betle* extract co-loaded for targeted anti-inflammatory therapy. The nano-herbosomes showed favourable physicochemical traits: particle size at nanoscale, significant entrapment efficiency, and stable zeta potential, indicating formulation stability and effectiveness. Spectroscopic and thermal characterization showed encapsulation was achieved without any chemical incompatibilities, and morphological examinations confirmed the presence of distinct spherical, polymer-coated vesicles. The release profiling *in vitro* demonstrated the intended stimuli-responsive behaviour of sustained and pH-sensitive release, especially at acidic pH levels simulating inflamed tissues. Significant increase in protein denaturation inhibition, membrane stabilization, nitric oxide and pro-inflammatory cytokine secretion from LPS macrophages suppression demonstrated enhanced activity of the nano-herbosomal formulation compared to free actives during anti-inflammatory evaluations.

5. References

1. Neu J,Walker WA. *Necrotizing enterocolitis*. N Engl J Med. 2011; 364(3):255-264. https://doi.org/10.1056/NEJMra1005408 PMid:21247316 PMCid:PMC3628622.
2. Jobe AH, Bancalari E. *Bronchopulmonary dysplasia*. Am J Respir Crit Care Med. 2001; 163(7):1723-1729.https://doi.org/10.1164/ajrccm.163.7.2011060 PMid:11401896.
3. Hagberg H, Mallard C, Ferriero DM, *et al*. The role of inflammation in perinatal brain injury. Nat Rev Neurol. 2015; 11(4):192-208. https://doi.org/10.1038/nrneurol.2015.13 PMid:25686754 PMCid: PMC4664161.
4. Bose C, Laughon M. Treatment of patent *Ductus arteriosus*. Semin Perinatol. 2007; 31(4):245-251. https://doi.org/10.1053/j.semperi.2007.05.006 PMid:17825673
5. Gupta SC, Patchva S, Aggarwal BB. Therapeutic roles of *curcumin*: lessons learned from clinical trials. AAPS J. 2013; 15(1):195-218. https://doi.org/10.1208/s12248-012-9432-8 PMid:23143785 PMCid: PMC3535097.
6. Rintu D, Shinjini M, Kaustab M, Pramathadhip P, Umesh PS, Banerjee ER. Antioxidant and anti-inflammatory activities of different varieties of *P. betle* leaf extracts (*P. betle* L.). J Nutr Food Sci. 2015; 5:415:1-5. https://doi.org/10.4172/2155-9600.1000415.
7. Sarkar A, Kumar KA, Pal A. Anti-inflammatory potential of *betel* leaf extract. Asian J Pharm Clin Res. 2014; 7(1):41-43.
8. Anand P, Kunnumakkara AB, Newman RA, Aggarwal BB. Bioavailability of *curcumin*: problems and promises. Mol Pharm. 2007; 4(6):807-818. https://doi.org/10.1021/mp700113r PMid:17999464.
9. Yanyu X, Yunmei S, Zhipeng C, Qineng P. The preparation of *silybin–phospholipid complex* and the study on its pharmacokinetics in rats. Int J Pharm. 2006; 307(1):77-82. https://doi.org/10.1016/j.ijpharm.2005.10.002 PMid:16289984.
10. Lee Y, Fukushima S, Bae YH. Heterogeneity of the enhanced permeability and retention (EPR) effect in tumor targeting. J Control Release. 2013; 172(2):632-639. https://doi.org/10.1016/j.jconrel.2013.09.026 PMid:24096014 PMCid: PMC3889175.
11. Khandelwal KR. Practical pharmacognosy: techniques and experiments. 19th ed. Pune: Nirali Prakashan; 2008.
12. Kokate CK, Purohit AP, Gokhale SB. Pharmacognosy. 49th ed. Pune: Nirali Prakashan; 2015.
13. Chattopadhyay I, Biswas K, Bandyopadhyay U, Banerjee RK. *Turmeric* and *curcumin*: biological actions and medicinal applications. Curr Sci. 2004; 87(1):44-53.
14. Priyadarsini KI. The chemistry of *curcumin*: from extraction to therapeutic agent. Molecules. 2014; 19(12):20091-20112. https://doi.org/10.3390/molecules191220091. PMid:25470276 PMCid: PMC6270789.
15. Jadhav VM, Thorat RM, Kadam VJ, Salaskar KR. Traditional medicinal uses of *Curcuma longa*: review. Pharma Rev. 2007; 5(6):137-140.
16. Mozafari MR. Liposomes: An overview of manufacturing techniques. Cell Mol Biol Lett. 2005; 10(4):711-719. doi:10.2478/s11658-005-0047-0.
17. Akbarzadeh A, Rezaei-Sadabady R, Davaran S, *et al*. Liposome: classification, preparation, and applications. Nanoscale Res Lett. 2013; 8(1):102. https://doi.org/10.1186/1556-276X-8-102 PMid:23432972 PMCid: PMC3599573.
18. Jain S, Jain NK. Lipid vesicular systems for delivery of phytoconstituents. Curr Drug Deliv. 2010; 7(4):265-275. doi:10.2174/156720110792006820
19. Pignatello R, Musumeci T, Basile L, Carbone C, Puglisi G. Polymeric nanoparticles for drug delivery: recent developments and future prospects. Expert Opin Drug Deliv. 2011; 8(7):871-885. https://doi.org/10.1517/17425247.2011.568936 PMid:21453189.
20. Mohammed MA, Syeda JTM, Wasan KM, Wasan EK. An overview of *chitosan nanoparticles* and its application in non-parenteral drug delivery. Pharmaceutics. 2017; 9(4):53. https://doi.org/10.3390/pharmaceutics9040053 PMid:29156634 PMCid: PMC5750659.
21. Danaei M, Dehghankhold M, Ataei S, *et al*. Impact of particle size and polydispersity index on the clinical applications of lipidic nanocarrier systems. Pharmaceutics. 2018; 10(2):57. https://doi.org/10.3390/pharmaceutics10020057 PMid:29783687 PMCid: PMC6027495.
22. Shoba G, Joy D, Joseph T, *et al*. Influence of *piperine* on the pharmacokinetics of *curcumin* in animals and human

volunteers. Planta Med. 1998; 64(4):353-356. https://doi.org/10.1055/s-2006-957450 PMid:9619120.
23. Jain AK, Thanki K, Jain S. Co-delivery of p-glycoprotein inhibitor and *curcumin* using polymeric nanoparticles: an approach for enhanced chemosensitization in cancer. J Pharm Sci. 2014; 103(2):674-682. https://doi.org/10.1002/jps.23791
24. Sharma A, Sharma US. Liposomes in drug delivery: progress and limitations. Int J Pharm. 1997; 154(2):123-140. https://doi.org/10.1016/S0378-5173(97)00135-X
25. Singh D, Rawat MSM, Semalty A, Semalty M. Development and characterization of a novel phytovesicular formulation of *curcumin* for transdermal delivery. Drug Dev Ind Pharm. 2010; 36(2):245-254. doi:10.3109/03639040903057163
26. Kaur R, Gulati M, Singh SK, *et al.* Development and characterization of phospholipid complex of *curcumin* for effective delivery. Drug Dev Ind Pharm. 2018; 44(9):1545-1557. doi:10.1080/03639045.2018.1461232.
27. Lu Y, Park K. Polymeric micelles and alternative nanonized delivery vehicles for poorly soluble drugs. Int J Pharm. 2013; 453(1):198-214. https://doi.org/10.1016/j.ijpharm.2012.05.052 PMid:22883694.
28. Lee ES, Gao Z, Bae YH. Recent progress in tumor pH targeting nanotechnology. J Control Release. 2008; 132(3):164-170. https://doi.org/10.1016/j.jconrel.2008.05.025 PMid:18547671.
29. Liu W, Zhai Y, Heng X, *et al.* Oral bioavailability of *curcumin*: problems and advancements. J Drug Target. 2016; 24(8):694-702. https://doi.org/10.3109/1061186X.2016.1157883 PMid:26942997.
30. Jain S, Jain AK, Umamaheshwari RB, Jain NK. Development of colonic delivery system for *curcumin*: a technical note. AAPS PharmSciTech. 2004; 5(4): e65. https://doi.org/10.1208/pt050465 PMid:15760062 PMCid: PMC2750490.
31. Korsmeyer RW, Gurny R, Doelker E, *et al.* Mechanisms of solute release from porous hydrophilic polymers. Int J Pharm. 1983; 15(1):25-35. https://doi.org/10.1016/0378-5173(83)90064-9
32. Patil SA, Belgamwar VS, Surana SJ. Solubility enhancement of *curcumin* using modified locust bean gum and chitosan. Indian J Pharm Educ Res. 2011; 45(2):136-142.
33. Mizushima Y, Kobayashi M. Interaction of anti-inflammatory drugs with serum proteins, especially with some biologically active proteins. J Pharm Pharmacol. 1968; 20(3):169-173. https://doi.org/10.1111/j.2042-7158.1968.tb09718.x PMid:4385045.
34. Shinde UA, Phadke AS, Nair AM, *et al.* Membrane stabilizing activity—a possible mechanism of action for the anti-inflammatory activity of Cedrus deodara wood oil. Fitoterapia. 1999; 70(3):251-257. https://doi.org/10.1016/S0367-326X(99)00030-1

Authors Contribution

Patil Sumesh Dnyaneshwar Conceptualized the study, designed the review framework, and performed the initial literature search. Borse Rahul Suresh Contributed to data curation, analysis of selected studies, and drafting major sections of the manuscript. Hiralben Mehta Provided critical revisions, supervised the project, and finalized the manuscript for submission. All authors have read and agreed to the published version of the manuscript.